Cavity pattern formation with incoherent light

Buljan, Hrvoje; Soljačić, Marin; Carmon, Tal; Segev, Mordechai

Cavity pattern formation with incoherent light

Hrvoje Buljan,[1,2] Marin Soljačić,[3] Tal Carmon,[1] and Mordechai Segev[1]
[1]*Physics Department, Technion-Israel Institute of Technology, Haifa 32000, Israel*
[2]*Department of Physics, Faculty of Science, University of Zagreb, PP 332, 10000 Zagreb, Croatia*
[3]*Physics Department, Massachusetts Institute of Technology, Cambridge, Massachusetts 02139, USA*
(Received 15 April 2003; revised manuscript received 15 May 2003; published 29 July 2003)

We study the propagation dynamics of an incoherent light beam circulating in a passive cavity containing noninstantaneous nonlinear media. It is shown that patterns form in this cavity in spite of spatial incoherence of the light. We show that the pattern formation process is always associated with two consecutive thresholds. The first (instability) threshold is unaffected by the cavity boundary conditions, whereas the second threshold is induced by the feedback through the interplay of nonlinear gain and cavity loss.

DOI: 10.1103/PhysRevE.68.016616 PACS number(s): 42.65.Tg

I. INTRODUCTION

Nonlinear optical systems with feedback and associated phenomena, such as pattern formation [1] and cavity solitons [2,3], have been continuously drawing attention for several reasons. On the fundamental side, the understanding of nonlinear optical phenomena contributes immensely to the understanding of nonlinear dynamical systems in general, and has a direct impact on other fields [4]. Equivalent nonlinear phenomena appear in various areas of physics, chemical, and biological systems [4]. From the applications standpoint, these systems can be engineered to perform as useful devices for switching, storing, and manipulating information [5]. The phenomenon of pattern formation refers to the fact that in an extended nonlinear medium, above a suitable threshold, any uniform intensity distribution of light becomes unstable, and splits into space (time) correlated domains [1]. In nonlinear optical cavities, patterns can assume a variety of forms: stripes, hexagons, rolls etc. [6]. Nonlinear optical cavities can also give rise to cavity solitons [2,3,5]. However, all previous studies of nonlinear optical cavities have considered only spatially coherent light [7].

Here we present the study of pattern formation in a nonlinear optical cavity with spatially incoherent light. The system is a passive ring cavity of length L_c, containing a nonlinear medium (crystal) of length $L \ll L_c$. The intensity structure from the output face of the crystal is attenuated by a factor ϵ and imaged to the input face of the crystal by using conventional optics. The light entering the cavity is partially spatially incoherent yet quasimonochromatic, with temporal coherence length l_{coh} much shorter than the cavity length: $L \ll l_{coh} \ll L_c$. The finesse of the cavity is low, of order one or less, which ensures that the temporal coherence length of the light is not increased by any filtering process in the cavity. Experimentally, this requirement can be achieved simply by making the length of the cavity large enough, since this reduces the separation between the resonant frequencies thereby decreasing finesse. The nonlinear medium has a noninstantaneous response; its response time is much longer than (i) the characteristic time of phase fluctuations across the beam and (ii) the average time of phase fluctuations between the beams from different cycles. The medium responds only to the time-averaged intensity [8,9]. This is the key physical mechanism responsible for the pattern formation in this *incoherent cavity*. Examples for noninstantaneous nonlinear media are photorefractive crystals [8], liquid crystals [9], polymers, etc.

The main goal of this paper is to analyze the early stage of pattern formation process in the incoherent cavity. By using the stability analysis of a uniform intensity beam in the cavity, it is shown that the pattern formation process is always associated with two consecutive thresholds which are determined by the degree of spatial coherence, the strength of the nonlinearity, and the cavity feedback parameter. At the first threshold the beam becomes unstable, as self-focusing overcomes diffusive tendency of spatially incoherent light. The second threshold occurs when the nonlinear gain overcomes the loss in a single pass. The first (instability) threshold is independent of the cavity boundary conditions, which is in contrast to the coherent cavities (e.g., see Ref. [10]), whereas the second threshold is an inherent cavity feature. As an interesting feature of our system, we point out that if the nonlinearity is at low (high) saturation, an increase in feedback leads to forward (backward) crossing over of the two thresholds, i.e., to switching the pattern on (off).

II. PROPAGATION EQUATIONS AND BOUNDARY CONDITIONS

For the analysis of the incoherent cavity, the quantities arising from coherence, such as the resonant frequencies (modes) of the cavity [11], are unimportant. Hence, the theoretical description cannot resort to the commonly used mean-field theory [11]. Instead, a new approach with new parameters (e.g., the degree of spatial coherence) has to be adopted.

We begin by deriving equations governing the dynamics. We assume that the light circulating through the cavity is linearly polarized. The slowly varying amplitude of the electric field cycling through the cavity for the jth time is described by a complex amplitude $\psi_j(x,z,t)$, where x denotes the spatial coordinate, z is the propagation axis, and t denotes time. The spatial coherence properties and intensity of the field cycling for the jth time through the cavity are described by the mutual coherence function $B_j(x_1,x_2,z) = \langle \psi_j(x_2,z,t)^* \psi_j(x_1,z,t) \rangle$ [12], where brackets $\langle \cdots \rangle$ de-

note the time average taken over the response time of the medium. Since the finesse of the cavity is low, and the temporal coherence length of the light l_{coh} is much smaller than the length of the cavity L, the phases of the fields that are circulated through the cavity a different number of times are mutually uncorrelated, that is, $\langle \psi_j^* \psi_l \rangle = 0$ for $j \neq l$.

Under the paraxial approximation [13], the propagation dynamics of the mutual coherence functions B_j within the nonlinear medium is given by an infinite set of coupled partial differential equations

$$\frac{\partial B_j}{\partial z} - \frac{i}{k}\frac{\partial^2 B_j}{\partial r\,\partial \rho} = \frac{ik}{n_0}\{\delta n(I_+) - \delta n(I_-)\}B_j(r,\rho,z), \quad (1)$$

where $j = 1,2,\ldots$. In Eq. (1), the new set of spatial coordinates is defined by $r = (x_1 + x_2)/2$ and $\rho = x_1 - x_2$, $I_\pm$ denotes the time-averaged intensity $I_\pm = \Sigma_l B_l(r \pm \rho/2,0,z)$, the nonlinear response of the material is $n^2(I) \simeq n_0^2 + 2n_0\delta n(I)$, and k is the wave number of the carrier (in the medium). In the feedback loop, the light is imaged from the $z = L$ face of the crystal to the incident plane $z = 0$. Hence, besides the propagation equations (1), the mutual coherence functions B_j are also subject to the boundary conditions

$$B_{j+1}(r,\rho,z=0) = \epsilon B_j(r,\rho,z=L), \quad (2)$$

where ϵ denotes the cavity feedback parameter. From Eq. (1), we see that diffraction is accounted for in the nonlinear part of the cavity [the term $ik^{-1}\partial^2 B_j/\partial r\,\partial\rho$]. The boundary conditions consider only losses since the conventional optical system in the feedback loop images light from the output to the input face of the crystal.

III. LINEAR STABILITY ANALYSIS OF A UNIFORM INTENSITY BEAM

To study the stability of the uniform intensity beam, we express the mutual coherence functions as

$$B_j(r,\rho,z) = B_j^{(0)}(\rho) + B_j^{(1)}(r,\rho,z), \quad (3)$$

where $B_j^{(1)}(r,\rho,z)$ denotes small perturbations upon the uniform intensity component $B_j^{(0)}(\rho)$. Boundary conditions (2) must be satisfied by the uniform intensity components $B_{j+1}^{(0)}(\rho) = \epsilon B_j^{(0)}(\rho)$ and by the small perturbations $B_{j+1}^{(1)}(r,\rho,0) = \epsilon B_j^{(1)}(r,\rho,L)$. From this, we express the uniform component of the jth cycle in terms of the uniform component of the incident beam, $B_j^{(0)}(\rho) = \epsilon^{j-1} B_1^{(0)}(\rho)$, and find the total uniform intensity of the light in the cavity, $I_{total} = \Sigma_l B_l^{(0)}(0) = I^{(0)}/(1-\epsilon)$; the intensity of the incident beam is denoted by $I^{(0)} = B_1^{(0)}(0)$. As long as perturbations are small enough, i.e., $|B_j^{(1)}(r,\rho,z)| \ll |B_j^{(0)}(\rho)|$, Eq. (1) can be linearized:

$$\frac{\partial B_j^{(1)}}{\partial z} - \frac{i}{k}\frac{\partial^2 B_j^{(1)}}{\partial r\,\partial\rho} = \frac{ik\kappa}{n_0}B_j^{(0)}(\rho)\sum_l \left\{ B_l^{(1)}\left(r + \frac{\rho}{2},0,z\right) - B_l^{(1)}\left(r - \frac{\rho}{2},0,z\right)\right\}, \quad (4)$$

where $\kappa = \partial\delta n(I)/\partial I|_{I=I_{total}}$. Equations (4) are linearized, however, they are still coupled. To uncouple Eq. (4), we seek their solution through the superposition of modes

$$B_j^{(1)}(r,\rho,z) = \epsilon^{j-1} M_1(r,\rho,z) + \sum_{l\geq 2} h_{jl} M_l(r,\rho,z), \quad (5)$$

where $h_{jl} = \delta_{jl-1} - \delta_{jl}$, and δ_{jl} denotes the Kronecker delta. From Eqs. (4) and (5), we find that the modes evolve according to

$$\frac{\partial M_j}{\partial z} - \frac{i}{k}\frac{\partial^2 M_j}{\partial r\,\partial\rho} = \delta_{1j}\frac{ik\kappa B_1^{(0)}(\rho)}{n_0(1-\epsilon)}\left\{ M_1\left(r + \frac{\rho}{2},0,z\right) - M_1\left(r - \frac{\rho}{2},0,z\right)\right\}. \quad (6)$$

Equation (6) for the first mode M_1 is equivalent to the equation describing modulation instability (MI) in a spatially incoherent single-pass system [14], which implies that the first mode M_1 can experience nonlinear gain and destabilize the beam. In contradistinction, since the right-hand side of Eq. (6) is zero for $j \geq 2$ [due to the term $\delta_{1j} = 0$], all other modes M_j, $j \geq 2$, satisfy equation describing the evolution of small perturbations in a *linear* medium; consequently, they do not experience any nonlinear gain.

Equation (6) can be solved with Fourier analysis. In order to satisfy condition $B_j(r,\rho,z) = B_j(r,-\rho,z)^*$, we express the modes as $M_j(r,\rho,z) = P_j(r,\rho,z) + P_j(r,-\rho,z)^*$, where

$$P_j(r,\rho,z) = \int_{-\infty}^{\infty}\int_{-\infty}^{\infty} d\alpha\, dK\, e^{g_j(\alpha)z}\hat{L}_j^\alpha(K)A_j(\alpha)e^{-iK\rho}e^{i\alpha r}. \quad (7)$$

Here, α denotes the spatial wave number, $g_j(\alpha)$ the growth rates, $A_j(\alpha)$ the amplitudes, and $\hat{L}_j^\alpha(K)$ the spatial coherence properties of the perturbations corresponding to the jth mode M_j. The functions $\hat{L}_j^\alpha(K)$ are normalized so that $\int dK \hat{L}_j^\alpha(K) = 1$. From Eqs. (6) and (7) for $j = 1$, and with the use of $\int dK \hat{L}_1^\alpha(K) = 1$, we obtain an implicit integral equation for the growth rate of the first mode $g_1(\alpha)$:

$$\frac{k\kappa}{n_0(1-\epsilon)}\int_{-\infty}^{\infty}\frac{h(K,\alpha)}{ig_1 + \dfrac{\alpha K}{k}}dK = -1, \quad (8)$$

where $h(K,\alpha) = \hat{B}_1^{(0)}(K + \alpha/2) - \hat{B}_1^{(0)}(K - \alpha/2)$, and $\hat{B}_j(K)$ denotes the Fourier transform of $B_j(\rho)$. The growth rate of the first mode $g_1(\alpha)$ can assume real values greater than zero. The growth rate of the nongrowing eigenmodes is purely imaginary: $g_j(\alpha) = iK\alpha/k$, for $j \geq 2$.

The boundary conditions $B_{j+1}^{(1)}(r,\rho,0) = \epsilon B_j^{(1)}(r,\rho,L)$ can be written as

$$\epsilon^j A_1(\alpha)\hat{L}_1^\alpha(K)[e^{g_1 L} - 1] = \sum_{l=2}^{\infty} a_{jl}A_l(\alpha)\hat{L}_l^\alpha(K), \quad (9)$$

where $j=1,2,\ldots$, $a_{jj}=\epsilon e^{g_2 L}$, $a_{jj+1}=-(\epsilon e^{g_2 L}+1)$, $a_{jj+2}=1$, and $a_{jl}=0$ otherwise. From Eq. (9), it follows that the coherence properties $\hat{L}_j(K)$ and amplitudes $A_j(\alpha)$ of the non-growing modes ($j\geqslant 2$) can be expressed in terms of the coherence properties $\hat{L}_1(K)$ and amplitude $A_1(\alpha)$ of the first mode. From Eqs. (6) and (7) for $j=1$, and by using $\int dK \hat{L}_1^{\alpha}(K)=1$, it follows that $\hat{L}_1^{\alpha}(K)$ is determined [via $h(K,\alpha)$] by the coherence of the source:

$$\hat{L}_1^{\alpha}(K)=-\frac{k\kappa}{n_0(1-\epsilon)}\frac{h(K,\alpha)}{ig_1+\dfrac{\alpha K}{k}}. \tag{10}$$

The perturbations upon the incident beam can be written as $B_1^{(1)}(r,0,0)=\int_{-\infty}^{\infty}A_{INC}(\alpha)e^{i\alpha r}d\alpha+\text{c.c.}$, and via boundary conditions as $B_1^{(1)}(r,0,0)=\Sigma_{j=1}^{\infty}[B_j^{(1)}(r,0,0)-\epsilon B_j^{(1)}(r,0,L)]$. From these two identities and Eqs. (5) and (7), we obtain

$$A_1(\alpha)=(1-\epsilon)\frac{A_{INC}(\alpha)}{1-\epsilon e^{g_1(\alpha)L}}. \tag{11}$$

From the analysis above, we conclude that the coherence properties of the source $B_1^{(0)}(\rho)$, and the perturbations $A_{INC}(\alpha)$ upon the incident beam, determine the coherence properties and the perturbations corresponding to the fields that circulate in the cavity. Although the linear stability analysis performed in Eqs. (3)–(11) resembles the linear stability analysis from Ref. [14], we emphasize that there is a significant difference. Namely, together with linearized propagation equations (4), here the solution has to obey the cavity boundary conditions [Eq. (2)], which results in a specific cavity threshold (to be explained below) that accompanies pattern formation in a cavity. Such a threshold does not have a counterpart in a single-pass system such as the one in Ref. [14]. We also emphasize that Eqs. (1)–(11) can be straightforwardly generalized to include $(2+1)D$ systems.

IV. THE INSTABILITY THRESHOLD

The linear stability analysis of the uniform intensity beam above is applicable for any type of input beam correlation statistics and nonlinearity. From now on we assume that the correlation statistics is given by Lorenzian in Fourier space, $\hat{B}_1^{(0)}(K)\sim(K^2+K_0^2)^{-1}$, and that the nonlinearity is $\delta n(I)=\gamma I/(1+I/I_S)$. In the limit $I_S\to\infty$, the nonlinearity is of Kerr type, and saturable otherwise. The nonlinear gain $g_1(\alpha)$ follows from Eq. (8)

$$|g_1(\alpha)|=-\theta|\alpha|+|\alpha|\sqrt{\frac{\kappa}{n_0}\frac{I^{(0)}}{1-\epsilon}-\left(\frac{\alpha}{2k}\right)^2}, \tag{12}$$

where $\theta=K_0/k$ denotes the degree of spatial coherence. From Eq. (10), we find the functional dependence of the maximally destabilizing perturbation α_{max} (pattern wave vector in the low visibility regime) on the degree of coherence θ and other parameters:

$$\frac{\alpha_{max}}{k}=\left(\frac{2\kappa I^{(0)}}{n_0(1-\epsilon)}-\frac{\theta^2}{2}-\sqrt{\frac{2\kappa I^{(0)}}{n_0(1-\epsilon)}\theta^2+\frac{\theta^4}{4}}\right)^{1/2}. \tag{13}$$

Furthermore, from Eq. (12), it follows that there exists a well-defined threshold at which the beam becomes modulationally unstable; if

$$\kappa I^{(0)}/(1-\epsilon)>\theta^2 n_0, \tag{14}$$

the beam is unstable.

We point out that the incoherent beam incident on the cavity is unstable if and only if the same beam with intensity enhanced by the factor $(1-\epsilon)^{-1}$ is unstable in a single-pass system [14]. The factor $(1-\epsilon)^{-1}$ simply reflects the increase of total intensity in the cavity due to feedback, $I_{total}=I^{(0)}/(1-\epsilon)$. Thus, below and at the instability threshold, one cannot distinguish from the cavity system with incident intensity $I^{(0)}$, and the single-pass system with intensity $I^{(0)}/(1-\epsilon)$. Physically, this equivalence is a consequence of the mutual incoherence between the fields of different cycles. The perturbations and the uniform parts of beams from different cycles do not interfere, but simply add up. This means that apart from the trivial enhancement of total intensity, the cavity boundary conditions do not affect the position of the MI threshold. This is also confirmed by the fact that the position of the instability threshold, given by inequality (14), does not depend on the length of the sample L, which is embedded in boundary conditions (2). This result is in a sharp contrast to coherent cavities [10], where the instability process is influenced by the boundary conditions through the interference of fields from different cycles.

V. THE CAVITY THRESHOLD

In contrast to the instability threshold, the boundary conditions, through the interplay of nonlinear gain and cavity loss, induce a transition from the low to high visibility pattern. To see this, we calculate the modulation depth of the intensity pattern. From Eqs. (5), (7), and (11), it follows that the intensity pattern at $z=L$ is

$$\sum_{i=1}^{\infty}B_i^{(1)}(r,0,L)=\int\frac{e^{g_1(\alpha)L}}{1-\epsilon e^{g_1(\alpha)L}}A_{INC}(\alpha)e^{i\alpha r}\,d\alpha+\text{c.c.} \tag{15}$$

From Eq. (15), we can estimate the modulation depth (visibility) $m=(I_{max}-I_{min})/(I_{max}+I_{min})$ of the pattern.

First, we calculate integral (15) numerically. We assume that the noise upon the incident beam does not have any preferential spatial frequency α, i.e., $|A_{INC}(\alpha)|$ is independent of α, while the phase of $A_{INC}(\alpha)$ is random. For the illustrations of the pattern visibility, we use the following parameters. The length of the nonlinear medium is $L=5$ mm, the wavelength of the carrier wave is $\lambda=488$ nm (in vacuum), and the linear part of the refractive index is $n_0=2.3$. The dependences of the modulation depth on the feedback ϵ and the strength of the nonlinearity $\Delta n=\gamma I^{(0)}$ are displayed in Figs. 1 and 2, respectively; solid lines rep-

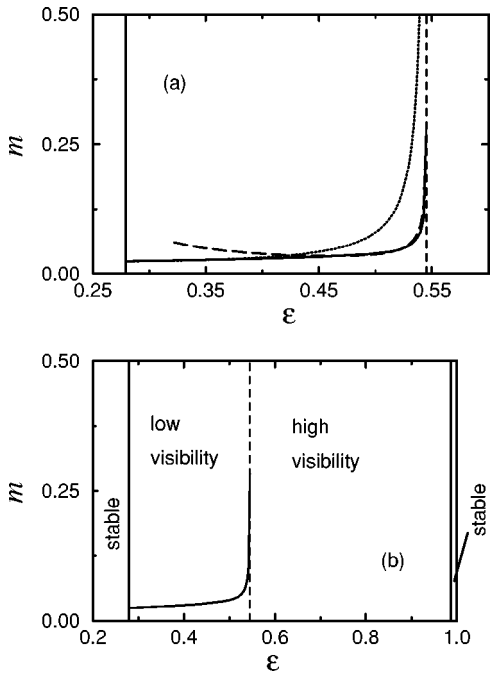

FIG. 1. The modulation depth m of the pattern vs the feedback parameter ϵ. Vertical solid (dashed) lines show the position of the first (second) threshold. Solid curves show m calculated numerically from Eq. (15). (a) The dotted curve represents $m_{\alpha_{max}}$ [see Eq. (16)], and the dashed curve represents modulation depth calculated from expression (18). (b) The region of the stable output, and of a low and high visibility pattern. For ϵ close to 1, the nonlinearity is highly saturated, and the pattern is switched off. The parameters used are $\Delta n = 10^{-4}$, $\theta = 0.0068$, and $I^{(0)}/I_S = 0.1$.

resent the values of m calculated numerically from integral (15). Vertical lines represent the positions of the thresholds as is explained in figure captions. From Figs. 1 and 2, we see that just after the instability threshold, the modulation depth grows until it comes close to the second threshold where the modulation depth experiences a sudden jump. This second

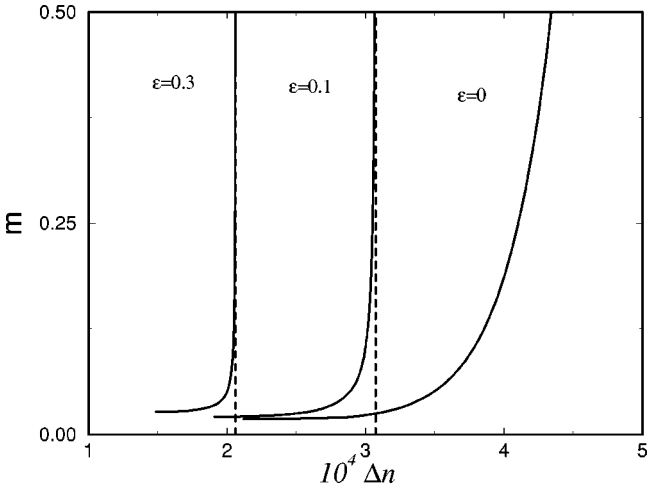

FIG. 2. The modulation depth vs $\Delta n = \gamma I^{(0)}$ for different values of ϵ; $\theta = 0.0096$, and $I_S = \infty$. m is shown from the instability threshold up to the cavity threshold (indicated by vertical dashed lines).

threshold is the cavity threshold which appears when the denominator of the integrand (15) becomes zero.

Before explaining the cavity threshold, let us gain more insight into the modulation depth of the pattern by analytical formulas. From Eq. (15), it follows that the maximally destabilizing perturbation α_{max} has the largest contribution to integral (15). The modulation depth of the maximally destabilizing perturbation α_{max} (not the whole pattern) is

$$m_{\alpha_{max}} \simeq C_1(1-\epsilon)\frac{e^{g_1(\alpha_{max})L}}{1-\epsilon e^{g_1(\alpha_{max})L}}, \tag{16}$$

where parameter C_1 corresponds to the strength of the small intensity perturbations upon the incident beam. The dotted curve in Fig. 1 displays the behavior of $m_{\alpha_{max}}$. We see that $m_{\alpha_{max}}$ describes well the trend of the modulation depth behavior in between the two thresholds, however, it diverges faster than the modulation depth calculated numerically.

A more accurate description can be achieved by approximately integrating expression (15). The growth rate $g(\alpha) = g_1(\alpha)$ can be Taylor expanded around the maximally destabilizing perturbation α_{max}, $g(\alpha) \simeq g(\alpha_{max}) + \frac{1}{2}g''(\alpha_{max}) \times (\alpha - \alpha_{max})^2$, and the integrand (15) is approximately

$$\frac{e^{g_1(\alpha)L}}{1-\epsilon e^{g_1(\alpha)L}} \simeq \frac{1}{\epsilon}\sum_{j=1}^{\infty} \epsilon^j e^{g(\alpha_{max})Lj} e^{-j/2|g''(\alpha_{max})|L(\alpha-\alpha_{max})^2}. \tag{17}$$

Approximate integration over α gives the following expression for the modulation depth:

$$m = C\frac{1-\epsilon}{\epsilon}\frac{\mathrm{Li}_{1/2}(\epsilon e^{g(\alpha_{max})L})}{\sqrt{|g''(\alpha_{max})|L}}, \tag{18}$$

where $Li_k(x) = \Sigma_{j=1}^{\infty} x^j/j^k$ denotes the polylogarithm function. We see that Eq. (18) for the modulation depth contains the term $1/\sqrt{|g''(\alpha_{max})|L}$ which expresses the spatial wave number selectivity. Namely, if the absolute value of the derivative $|g''(\alpha_{max})|$ is larger, integrand (17) will be more peaked around α_{max}, and only a small number of spatial frequencies close to α_{max} will contribute to the pattern. The functional dependence of the modulation depth from Eq. (18) on the feedback is displayed by a dashed curve in Fig. 1. Evidently, the functional form (18) does not increase monotonically from the first to the second threshold but has a minimum. This is a consequence of the spatial wave number selectivity term $1/\sqrt{|g''(\alpha_{max})|L}$. Thus, the functional form (18) can be used to describe the modulation depth only from that minimum up to the second threshold, i.e., when $|g''(\alpha_{max})|L$ becomes sufficiently large. From Fig. 1, we observe that the functional form (18) gives a good description for the behavior of the modulation depth below the second threshold. In Fig. 1, the parameter C is chosen such that the minimum of the curve from expression (18) intersects the numerically calculated curve for the modulation depth.

Now we explain the cavity threshold. In the cavity, the output pattern, with preferred periodicity determined by α_{max}, is imaged (with some loss) to the input plane, thus affecting the output pattern. From the denominator in Eq. (15), it follows that the modulation depth of the intensity pattern is determined by the relation between the nonlinear gain and cavity loss. If the nonlinear gain is smaller than the cavity loss, the modulation depth at the input is small enough, so that the pattern at the input is regarded as noise with preferential periodicity determined by α_{max}. However, if the nonlinear gain is larger than the cavity loss, the intensity structure at the input is more than just preferential noise; this structure guides the light from the input beam into its shape. This significantly differs from the single-pass MI, where the modulation depth at the input is always small, and the pattern builds from small noise [14]. From Figs. 1 and 2, we see that the feedback of the maximally destabilizing perturbation induces a rapid increase of the modulation depth, which is referred to as the cavity threshold; it occurs approximately when the nonlinear gain becomes equal to the cavity loss, i.e., when $\epsilon \exp g_1(\alpha_{max})L=1$. The transition will be sharper for larger values of the feedback parameter ϵ (see Fig. 2). This threshold is analogous to that in many feedback systems with gain (e.g., see Ref. [15]). The behavior of the intensity pattern in between the two thresholds corresponds to noisy precursors in one-dimensional patterns observed in Ref. [16].

We note that the features of the intensity structure above the cavity threshold cannot be determined from the stability analysis of Sec. III. However, this analysis shows that formation of any such structure is preceded by the two consecutive thresholds, and it predicts the positions of these thresholds in parameter space spanned by Δn, θ, and ϵ (see Fig. 3). From inequality (14), it follows that the increase of coherence and/or the strength of the nonlinearity always leads to pattern formation. The dependence of the stability on the feedback ϵ depends on the saturation of the medium. If the medium is Kerr, or in the regime of low saturation $I^{(0)}(1-\epsilon)^{-1}I_S^{-1} \ll 1$, the increase of feedback acts destabilizing. However, if the medium is in the regime of high saturation $I^{(0)}(1-\epsilon)^{-1}I_S^{-1} \gg 1$, then the increase of feedback leads to the stabilization of the beam. Thus, as an interesting feature of the cavity system, we show that in the limit of low (high) saturation, the increase of feedback leads to switching the pattern on (off) [see Figs. 1(b) and 3].

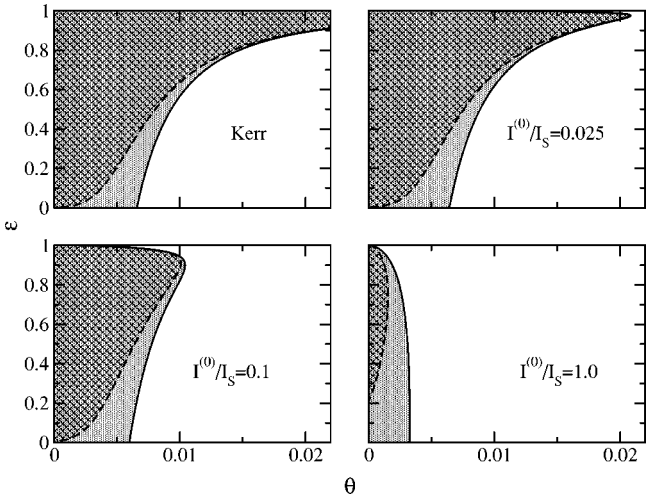

FIG. 3. The positions of the modulation instability threshold (solid line) and the cavity threshold (dashed line) in the (θ,ϵ) plane depending on the saturation intensity I_S; $\Delta n=10^{-4}$. White (cross-hatched) region denotes stable output (pattern, respectively).

VI. CONCLUSION

In conclusion, we have analyzed the early stage of pattern formation process in a nonlinear optical cavity with incoherent light. The nonlinear medium within the cavity has a noninstantaneous response, that is, it is unable to follow fast random fluctuations of incoherent light. We have demonstrated that two consecutive thresholds always accompany the process of pattern formation. In contrast to the coherent cavity cases [10], the instability threshold is unaffected by the incoherent cavity boundary conditions. The second (cavity) threshold is determined by the interplay of nonlinear gain and cavity loss. It appears when the nonlinear gain in single pass overcomes the cavity loss. For future work on incoherent optical cavities, such as the one described here, we envision the study of incoherent cavity solitons, whose features are yet to be determined.

ACKNOWLEDGMENTS

This work was supported by the German-Israeli DIP project, the Israeli Science Foundation, and is part of the MURI program on optical spatial solitons. H.B. acknowledges support from the Lady Davis Foundation.

[1] F.T. Arecchi, S. Boccaletti, and P. Ramazza, Phys. Rep. **318**, 1 (1999).

[2] W.J. Firth and G.K. Harkness, in *Spatial Solitons*, edited by S. Trillo and W. Torruellas (Springer-Verlag, Berlin, 2001), Chap. 13, pp. 343–358; C.O. Weiss *et al.*, in *Spatial Solitons*, edited by S. Trillo and W. Torruellas (Springer-Verlag, Berlin, 2001), Chap. 15, pp. 395–416.

[3] W.J. Firth and A.J. Scroggie, Phys. Rev. Lett. **76**, 1623 (1996).

[4] G. Nicolis, *Introduction to Nonlinear Science* (Cambridge University Press, Cambridge, 1995); H. Haken, *Synergetics: An Introduction* (Springer-Verlag, Berlin, 1977).

[5] S. Barland *et al.*, Nature (London) **419**, 699 (2002); M. Brambilla *et al.*, Phys. Rev. Lett. **79**, 2042 (1997); V.B. Taranenko *et al.*, Phys. Rev. A **61**, 063818 (2000).

[6] W.J. Firth *et al.*, Phys. Rev. A **46**, R3609 (1992); W.J. Firth and A.J. Scroggie, Europhys. Lett. **26**, 521 (1994); K. Staliunas *et al.*, Phys. Rev. A **51**, 4140 (1995); Phys. Rev. Lett. **79**, 2658 (1997); G.L. Oppo *et al.*, Phys. Rev. A **49**, 2028 (1994); S.J. Jensen *et al.*, Phys. Rev. Lett. **81**, 1614 (1998).

[7] In fact, almost all previous studies on pattern formation in

optical cavities considered cases where the light was *both spatially and temporally coherent*. There are only two exceptions. The first relates to some of the single-mirror feedback systems—those with the distance between the mirror and nonlinear medium much larger than l_{coh} [R. MacDonald *et al.*, Opt. Commun. **89**, 289 (1992)]; The second is a recent study [T. Carmon *et al.*, Phys. Rev. Lett. **89**, 183902 (2002)] with a passive nonlinear ring cavity with $l_{coh} \ll L_c$. We emphasize that the light in both of these studies was spatially coherent, in contrast to our current study with spatially incoherent light.

[8] M. Mitchell *et al.*, Phys. Rev. Lett. **77**, 490 (1996); D.N. Christodoulides *et al.*, *ibid.* **78**, 646 (1997); M. Mitchell *et al.*, *ibid.* **79**, 4990 (1997).

[9] M. Peccianti and G. Assanto, Opt. Lett. **26**, 1791 (2001).

[10] S. Coen and M. Haelterman, Phys. Rev. Lett. **79**, 4139 (1997); M. Haelterman, S. Trillo, and S. Wabnitz, Opt. Lett. **17**, 745 (1992).

[11] L.A. Lugiato and R. Lefever, Phys. Rev. Lett. **58**, 2209 (1987); L.A. Lugiato and C. Oldano, Phys. Rev. A **37**, 3896 (1988).

[12] L. Mandel and E. Wolf, *Optical Coherence and Quantum Optics* (Cambridge University Press, New York, 1995).

[13] V.V. Shkunov and D. Anderson, Phys. Rev. Lett. **81**, 2683 (1998).

[14] M. Soljačić *et al.*, Phys. Rev. Lett. **84**, 467 (2000); D. Kip *et al.*, Science **290**, 495 (2000).

[15] S.G. Lipson, H. Lipson, D.S. Tannhauser, *Optical Physics* (Cambridge University Press, Cambridge, 1995), p. 431.

[16] G. Agez, C. Szwaj, E. Louvergneaux, and P. Glorieux, Phys. Rev. A **66**, 063805 (2002).